Indian Journal of Chemical Technology
Vol. 30, January 2023, pp. 111-116
DOI: 10.56042/ijct.v30i1.66216

Triazole-based C3-symmetric multivalent dendritic architecture as Cu(II) ion sensor

Preeti Yadav[1,2], Badri Parshad[1,3], Krishna[1], Antara Sharma[1], Rita Kakkar[1] & Sunil K Sharma*[1]

[1]Department of Chemistry, University of Delhi, Delhi 110 007, India

[2]Department of Chemistry, Kalindi College, University of Delhi, New Delhi, India

[3]Wellman Center for Photomedicine, Massachusetts General Hospital, Harvard Medical School, Boston, MA 02129, USA

E-mail: sksharma@chemistry.du.ac.in

Received 5 September 2022; accepted 2 December 2022

C3-symmetric triazole-based multivalent dendritic architecture having uniform aromatic core and branches has been employed to study its metal binding ability towards Cr(III), Mn(II), Fe(III), Co(II), Ni(II), Cu(II) and Zn(II) ions. The dendritic architecture is found to exhibit a high affinity for Cu(II) ions and formed a solid complex with a blue shift in the dd-band of Cu(II) chloride. X-band EPR spectra at low temperature has supported a distorted tetrahedral geometry for the complex. The complex has displayed quasi-reversible redox waves in cyclic voltammetry (CV). DFT calculations have shown that Cu(II) has a high affinity for the dendritic structure, leading to high complexation energies of the order of -25 eV, showing that the complexation reactions are highly exothermic. The binding constant (K) for the Cu(II) complex has been determined using a fluorescence titration method.

Keywords: Binding constant, C3-symmetric, Cu-complex, Dendritic architecture, Metal sensor

Within the field of supramolecular chemistry, multivalency is a powerful and versatile technique as it confers unique thermodynamic and kinetic behaviour onto supramolecular complexes[1-5]. Coupled with the surge of interest in the development of techniques for the selective sensing/formation of metal complexes for various applications, our interest is in the application of macromolecules that possess multiple potential binding sites which can lead to multivalency effects and strengthen their binding affinity for selective cations. In this perspective, multivalent dendritic scaffolds that are three-dimensional macromolecular structures originating from a central core molecule and surrounded by multiple branches and surface units found to play significant role as effective sensing platform due to their better chelating efficiency caused by multivalent binding sites[6-8].

These dendritic structures exhibit a high degree of molecular uniformity, narrow molecular weight distribution, tuneable size and shape characteristics, as well as multivalency and provide ideal scaffold as host molecule due to presence of internal cavities and multiple functionalities[9-10]. Moreover, the design and construction of dendritic architectures through azide-alkyne click chemistry proved to be an effective approach in macromolecular chemistry[11-14]. The interdendritic [1,2,3]-triazole heterocycles resulting from the click approach act as coordination sites for metal ions[15]. The *N3* and *N2* of triazole ring are suitable for co-ordination to transition metals[16-18]. Such metal binding properties of triazole-based architectures have been used in the field of catalysis to carry out a number of carbon-carbon bond formation reactions[19-21]. Moreover, triazole-based dendritic scaffolds have found numerous applications such as fluorophores, chemosensors, charge-transfer agents, pathogen inhibitors and nanocarriers[22-27].

We have earlier synthesized symmetrical aromatic triazole-based dendritic architecture (G1) carrying the multiple triazole rings as well as hydroxyl groups[28]. Phloroglucinol, 3-bromopropyne and glycerol were used as starting materials and these were suitably modified so as to synthesize G1 by following the Williamson ether synthesis and Huisgen azide-alkyne 1,3-dipolar cycloaddition reaction (click chemistry approach).

The complex forming ability of the G1 was investigated by using chloride salts of Cr(III), Mn(II), Fe(III), Co(II), Ni(II), Cu(II) and Zn(II), in methanol. The synthesized dendritic architecture efficiently form the solid complex with Cu(II), which causes blue shift

in the dd-band of Cu(II) chloride salt. The complex formed was characterized by EPR and cyclic voltammetry.

Experimental Section

Materials

All the chemicals and reagents were procured from Spectrochem Pvt. Ltd., India and Sigma-Aldrich Chemicals, USA. The organic solvents were dried and distilled prior to their use. Reactions were monitored by precoated TLC plates (Merck silica gel $60F_{254}$); the spots were visualized either by UV light, or by staining with ceric solution.

Instruments

Infrared spectra were recorded on a Perkin-Elmer FT-IR model 9 spectrometer. UV-Visible absorption spectra were recorded using a Cary-300 UV-Vis spectrophotometer from Agilent-Technologies. Emission spectra were recorded using a Varian Cary Eclipse Fluorescence spectrophotometer (Cary-300). A quartz cuvette of 1 cm path-length was used to record absorption and emission spectra. The cyclic voltammetric measurements were carried out using a BAS CV 50 W electrochemical analysis system. Cyclic voltammograms of complexes were recorded in DMF:DMSO (3:1) with tetra-*n*-butylammonium perchlorate (TBAP) 0.1 M as supporting electrolyte. A three electrode configuration composed of Pt working electrode 3.1 mm^2 area, a Pt wire counter electrode, and an $Ag/AgNO_3$ reference electrode were used for the measurement. The reversible one electron Fc^+/Fc couple in above solvent system has an $E_{1/2}$ of 59.5 mV versus $Ag/AgNO_3$ electrode. Solution state EPR spectra were recorded on an X-band ESR-JEOL Spectrometer at liquid nitrogen temperature (77K) in dimethyl sulfoxide (DMSO) at IIT Bombay, India.

Fluorescence titration method

For the measurement of the binding constant (K) and the number of binding sites (n), the fluorescence titration method was used. The fluorescence titration of the Cu^{2+} ion was carried out using a solution of 0.83 mM of compound G1 in methanol. First the emission spectrum of G1 is recorded by exciting at wavelength 267 nm and setting the excitation and emission slit 10. This gives the value of I_o, which is the maximum emission intensity at 371 nm for G1, and with the addition of increasing concentrations of Cu^{2+}, emission intensity at 371 nm gradually decreases. A plot of $\log[(I_o - I)/I]$ as a function of the $\log[Cu^{2+}]$, gives the intercept and slope, from which the binding constant and the number of binding sites were calculated by using the following equation (1)[29].

$$\log[(I_o\text{-}I)/I] = \log K + n \log[Cu^{2+}] \quad \ldots(1)$$

Where, I_o = Intensity of G1 in absence of Cu^{2+}
I = Intensity of G1 in presence of Cu^{2+}
K = Binding constant
n = Number of binding sites

Procedure for the synthesis of G1-Cu complex

To a solution of G1 (100 mg, 0.17 mmol) in methanol (10 mL), the copper chloride salt (115.34 mg, 0.68 mmol) in methanol (10 mL) was added, then precipitate started forming, the reaction mixture was stirred for additional 2 h at room temperature. The precipitate formed was filtered, washed with methanol (2 × 10 ml) and dried to obtain G1-Cu complex.

Computational details

First-principles density functional (DF) calculations were performed using DMol[3] in the Materials Studio package[30]. A numerical basis set of double zeta quality plus polarization functions (DNP), which is the numerical equivalent of the Gaussian basis, 6-31G**, was used. The cores were treated using DFT Semilocal Pseudo-Potentials (DSPP), specifically designed for DFT calculations[31]. The GGA-PBE functional was employed in the calculations[32]. Spin-unrestricted calculations were performed using a Fermi broadening of 0.005 Ha[33]. The convergence criteria in energy, force, and displacement were set to 2×10^{-5} Ha, 0.004 Ha/Å, and 0.005 Å, respectively. A fine integration grid was used.

The geometries of the various structures were fully optimized, without restrictions, using delocalized internal coordinates[34, 35]. Bond orders were computed using Mayer's procedure[36]. The reported partial atomic charges are those obtained by Hirshfeld partitioning[37].

The complexation energies (E_{cmplx}) were calculated using the equation (2):

$$E_{cmplx} = E_{Cu^{2+}G1} - (E_{Cu^{2+}} + E_{G1}) \quad \ldots(2)$$

Where, $E_{Cu^{2+}G1}$ is the energy of the complex of G1 with Cu^{2+}, $E_{Cu^{2+}}$ and E_{G1} are the total energies of the isolated copper ion ($^2S_{1/2}$) and G1, respectively.

Results and Discussion

The G1 dendritic architecture having symmetrical aromatic core synthesized from phloroglucinol and

azido glycerol were studied for metal binding applications using chloride salts of different transition metals (Fig. 1). Out of the studied metal salts, Cu(II) binds efficiently with the G1 with remarkable change in emission spectra[38]. The dendritic architecture formed the solid complex with Cu(II), which led to a blue shift in dd-band of Cu(II) chloride salt.

Metal binding study by emission spectroscopy

The metal binding potential of the G1 was studied using its emission spectra. The addition of 0.1 equivalent of metal chloride [Cr(III), Mn(II), Fe(III), Co(II), Ni(II), Cu(II) and Zn(II)], caused the quenching of emission intensity at 371 nm for G1. A significant quenching of emission intensity was observed on addition of Cu(II) to G1, however a very low to moderate quenching was observed with other metal salts (Fig. 2).

The triazole ring nitrogens are reported to form complex with Cu(II) ion and the subsequent quenching in emission intensity of G1, in the presence of Cu(II) chloride, was used to estimate the binding constant (K) and the number of binding sites (n). The binding constant K and value of 'n' for G1 were estimated to be 7.015 × 10^{10} M^{-1} and 1.99, respectively (Fig. 3). These results suggest a stronger affinity for the synthesized molecule for Cu(II) as compared to PAMAM dendrimers[39] and chitin polymers[40] that exhibit a moderate affinity of 10^3-10^4 M^{-1} for Cu(II).

The detection limit for the copper ion by G1 was calculated from the titration data according to the reported method[41-43] by plotting a graph between normalized fluorescence intensity, $(I_{max}-I)/(I_{max}-I_{min})$ as a function $\log[Cu^{2+}]$ at 371 nm (Fig. 3). The intercept at the ordinate axis corresponds to the detection limit, for copper ion, this was found to be 0.13 μM.

Characterization of Cu-complex by absorption spectra, elemental analysis and IR spectra

Cu(II) complex of G1 was synthesized by mixing the solutions of G1 and copper chloride (4 eq.) in methanol. By mixing the two solutions at room temperature, a precipitate of green colored complex was obtained. While comparing the UV-Vis spectrum of these precipitates with copper chloride solution in

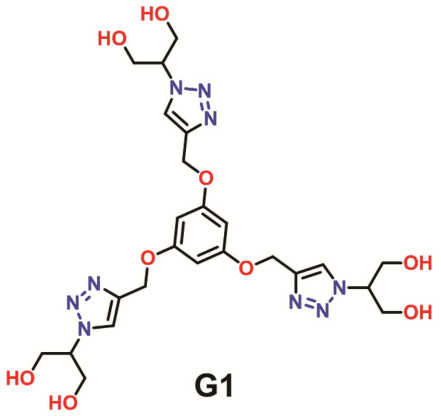

Fig. 1 — Molecular structure of G1 dendritic architecture having multiple triazole and hydroxyl groups.

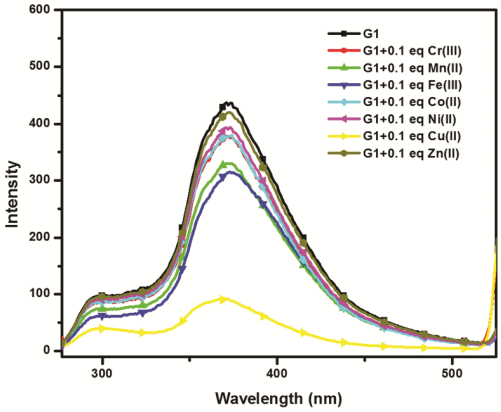

Fig. 2 — Emission spectra of G1 (1.69 mM) in the presence of different metal ions (0.1 equivalent) in methanol.

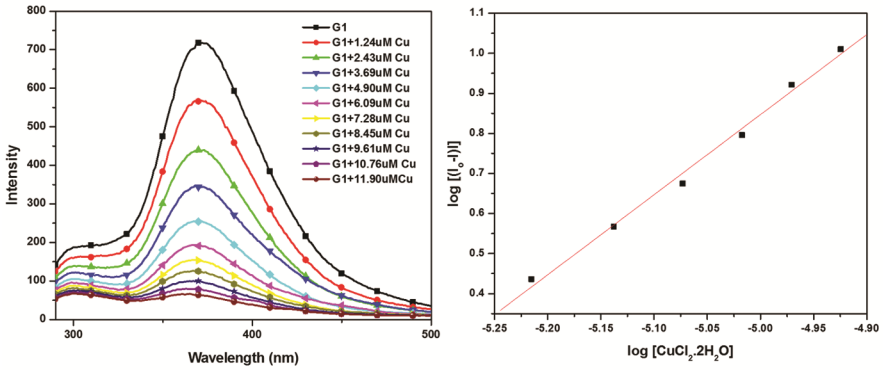

Fig. 3 — Emission spectrum of G1 with incremental addition of Cu^{2+} solution and a plot of $\log[(I_o - I)/I]$ as a function of the $\log[Cu^{2+}]$ in methanol.

water, a blue shift was observed in absorbance spectra of the G1-Cu complex (Fig. 4). The copper chloride in water reported to exhibit a weak dd-band at 819 nm[44, 45], which get shifted to 755 nm for the G1-Cu Complex.

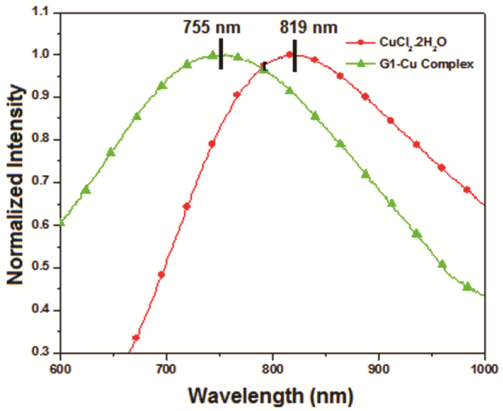

Fig. 4 — The observance of blue shift in absorption spectrum of copper chloride in water on complex formation with G1.

The elemental analysis data of G1 copper complex (G1-Cu Complex) was found to be quite close to 1:2 complex as shown in Fig. 5.

In the IR spectrum of G1, the bands observed at 1564.34 cm^{-1} and 1597.00 cm^{-1} are attributed to the *v* (C-N) of *N3* and *N1* of 1,2,3-triazole ring (Fig. 6). On complex formation the former band get shifted towards higher value, indicating the participation of *N3* of triazole ring (Fig. 6). The bands at 1053.18 and 1155.72 cm^{-1} are assigned for *v* (C-O) and *v* (N=N) stretch, respectively.

On complex formation *v* (N=N) stretch get shifted to higher value. These results suggest the participation of *N3* in complex formation of G1 with Cu(II) ion.

Electron Paramagnetic Resonance (EPR) data

The X-band EPR data of the copper(II) complex have been recorded at liquid nitrogen temperature in

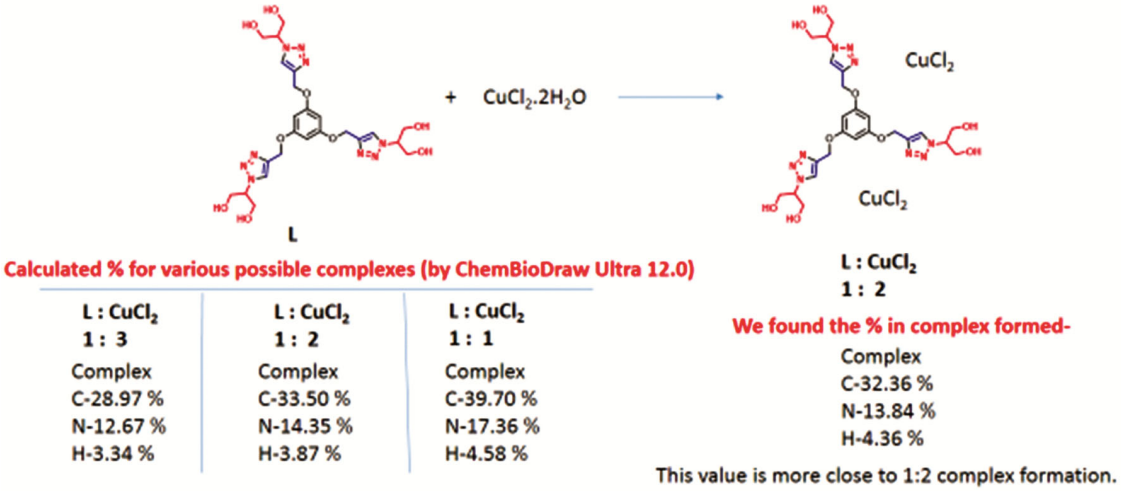

Fig. 5 — Elemental analysis data of G1-Cu Complex showing the relative percentage of C, N and H atoms.

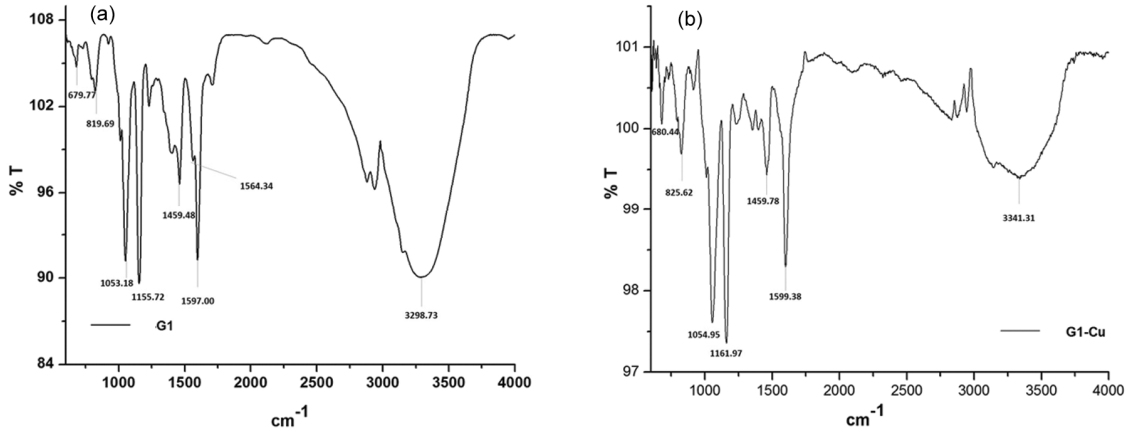

Fig. 6 — IR spectra of (a) G1 and (b) G1-Cu complex.

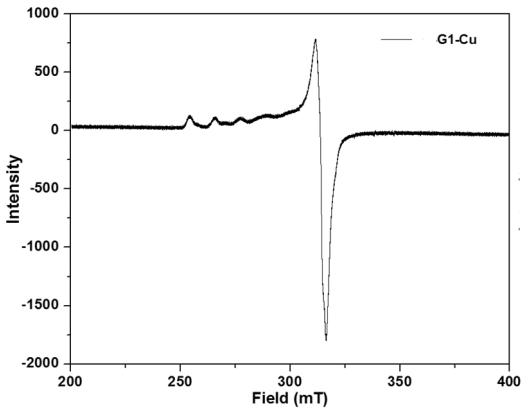

Fig. 7 — EPR spectrum of G1-Cu Complexes.

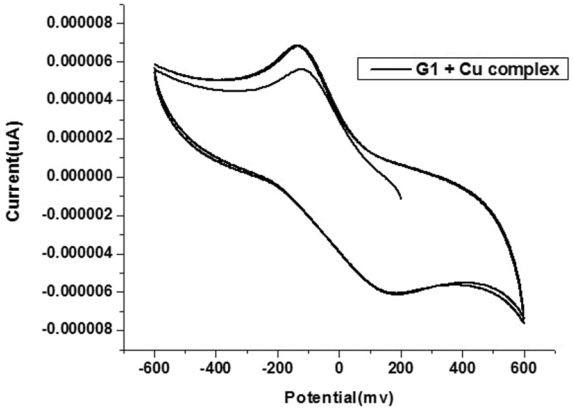

Fig. 8 — Cyclic voltammogram in DMF:DMSO (3:1) of G1-Cu complex at scan rate 200 mV/s.

Table 1 — EPR spectral parameters of the complexes.

Complex	$g_{//}$	$g_{\perp}$	$10^{-4} \times A_{//}$ (cm^{-1})	$10^{-4} \times A_{\perp}$ (cm^{-1})	$g_{//}/A_{//}$ (cm)
G1-Cu	2.4023	2.0805	110	48	218

DMSO, and EPR spectral parameters of the complexes are given in Table 1. The complex showed four $g_{//}$ and one $g_{\perp}$ components (Fig. 7). The ratio $g_{//}/A_{//}$ can be used to predict the geometry adopted by copper complexes, its value was calculated to be 218 cm for G1-Cu complex, falls in the range of 135-258 cm[46], indicating the distorted tetrahedral complexes. The $g_{//} > g_{\perp}$ and $A_{//} > A_{\perp}$ indicates that the complexes have the $d_{x^2-y^2}$ ground state.

Cyclic-voltammetry study

In cyclic voltammetry study, the G1-Cu complex displays quasi-reversible redox waves due to the Cu(II)/Cu(I) reduction process with $E_{1/2}$ value at 4.5 mV, while the value of Ipc/Ipa ratio found to be 0.91[47]. The peak potential is dependent on the scan rate, which further support the quasi-reversibility of the system (Fig. 8).

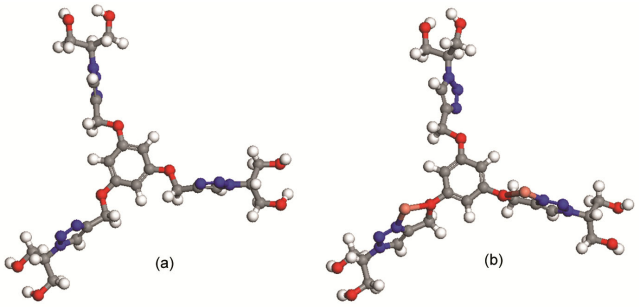

Fig. 9 — Optimized structure of (a) G1 and (b) Complex of G1 with two copper ions. Colour scheme: Carbon: Gray, Nitrogen: blue; Oxygen: Red; Hydrogen: White.

Computational studies

The structure of the G1 architecture was first energy minimized (Fig. 9(a)).

Since the experimental results had shown the involvement of a triazole nitrogen and an oxygen atom in complex formation, the Cu(II) ion was placed in the vicinity and the structure was geometry optimized. The complexation energy is very high (-17.64 eV), showing that the complexation reaction is highly exothermic. Placement of another copper ion yielded the complex shown in Fig. 9(b). The complexation energy for the second step is also high (-7.80 eV), making the overall complexation very high and negative (-25.44 eV). The complex is rather asymmetric, and the two Cu-O distances are 2.361 and 2.228 Å, whereas the Cu-N distances are 1.887 and 1.898 Å, respectively, forming two five membered rings, as shown in Fig. 9(b). An attempt to add a third Cu(II) ion failed. It may be concluded that G1 can complex up to two Cu(II) ions with a total complexation energy of -25.44 eV, in agreement with experiment.

Conclusion

Triazole-based C3-symmetric architecture has been investigated for metal sensing potential. The metal sensing potential of the G1 is studied using UV-Vis and emission spectroscopy. The investigated dendritic architecture exhibit high selectivity towards Cu(II) ions while a low to moderate affinity has been observed for other ions e.g. Cr(III), Mn(II), Fe(III), Co(II), Ni(II), Cu(II), and Zn(II). The studied dendritic architecture form the solid complex with Cu(II), which led to a blue shift in dd-band of Cu (II) chloride. The binding constants and number of binding sites of G1 with Cu(II) chloride have been calculated by fluorescence titration curve and are found to be 7.015×10^{10} M^{-1} and 1.99, respectively.

The EPR data suggests that the complex has tetragonally distorted geometry and cyclic voltammeteric study suggested it to be is a quasi-reversible system. DFT calculations have shown that Cu(II) has a high affinity for the dendritic structure, leading to high complexation energies of the order of -25 eV, thus supporting the fact that the complexation reactions are highly exothermic. This result in short Cu-O and Cu-N bonds. This is in agreement with the present experimental results. This study may find applications in the sensing/trace detection of Cu(II) ions in the solution and open up further avenues for biomedical and environmental applications.

Conflicts of interest

There are no conflicts to declare.

Acknowledgements

Financial support from the Department of Science and Technology, Government of India are gratefully acknowledged. We thank Council of Scientific and Industrial Research (CSIR) for awarding JRF/SRF to PY & BP.

References

1 Mammen M, Choi S K & Whitesides G M, *Angew Chem Int Ed*, 37 (1998) 2754.
2 Smeijers A F, Pieterse K, Hilbers P A J & Markvoort A J, *Macromolecules*, 52 (2019) 2778.
3 Fasting C, Schalley C A, Weber M, Seitz O, Hecht S, Koksch B, Dernedde J, Graf C, Knapp E W & Haag R, *Angew Chem Int Ed*, 51 (2012) 10472.
4 Lotfi B, Tarlani A, Akbari-Moghaddam P, Mirza-Aghayan M, Peyghan A A, Muzart J & Zadmard R, *Bio Bioelectron*, 90 (2017) 290.
5 Xianyu Y, Dong Y, Zhang Z, Wang Z, Yu W, Wang Z & Chen Y, *Bio Bioelectron*, 155 (2020) 112106.
6 Viltres H, López Y C, Leyva C, Gupta N K, Naranjo A G, Acevedo–Peña P, Sanchez-Diaz A, Bae J & Kim K S, *J Molecular Liquids,* 334 (2021) 116017.
7 Luan L, Tang B, Liu Y, Xu W, Liu Y, Wang A & Niu Y, *Langmuir,* 38 (2022) 698.
8 Wang Q, Zhu S, Xi C & Zhang F, *Frontiers Chem*, 10 (2022) Please give me pages number.
9 Barman S R, Nain A, Jain S, Punjabi N, Mukherji S & Satija J, *J Mater Chem B*, 6 *(*2018) 2368.
10 Wang J, Li B, Qiu L, Qiao X & Yang H, *J Biological Eng*, 16 (2022) 1.
11 Arseneault M, Wafer C & Morin J F, *Molecules*, 20 (2015) 9263.
12 Sumerlin B S & Vogt A P, *Macromolecules*, 43 (2010) 1.
13 Niu L, Song N, Wang X & Ding S, *Macromol Rapid Commun,* 29 (2022) 2200375.
14 Tiwari V K, Mishra B B, Mishra K B, Mishra N, Singh A S & Chen X, *Chem Rev*, 116 (2016) 3086.
15 Wang L, Kiemle D J, Boyle C J, Connors E L & Gitsov I, *Macromolecules*, 47 (2014) 2199.
16 Urankar D, Pinter B, Pevec A, De Proft F, Turel I & Košmrlj J, *Inorg Chem*, 49 (2010) 4820.
17 Crowley J D & Gavey E L, *Dalt Trans*, 39 (2010) 4035.
18 Kilpin K J, Gavey E L, McAdam C J, Anderson C B, Lind S J, Keep C C, Gordon K C & Crowley J D, *Inorg Chem*, 50 (2011) 6334.
19 Diallo A K, Ornelas C, Salmon L, Ruiz Aranzaes J & Astruc D, *Angew Chem Int Ed*, 46 (2007) 8644.
20 Ornelas C, Ruiz Aranzaes J, Cloutet E, Alves S & Astruc D, *Angew Chem Int Ed*, 46 (2007) 872.
21 Shiri P & Amani A M, *Monatshefte für Chemie-Chem Monthly,* 152 (2021) 367.
22 Thomas B, Yan K C, Hu X L, Donnier-Maréchal M, Chen G R, He X P & Vidal S, *Chem Soc Rev*, 49 (2020) 593.
23 Kumar S, Ma S, Mohan B, Li S & Ren P, *Inorg Chem,* 61 (2022) 14778.
24 Jarowski P D, Wu Y L, Schweizer W B & Diederich F, *Org Lett*, 10 (2008) 3347.
25 Brunel D & Dumur F, *New J Chem*, 44 (2020) 3546.
26 Mittal A, Prasad S, Mishra P K, Sharma S K & Parshad B, *Mater Adv,* 2 (2021) 3459.
27 Parshad B, Prasad S, Bhatia S, Mittal A, Pan Y, Mishra P K, Sharma S K & Fruk L, *RSC Adv*, 10 (2020) 42098.
28 Parshad B, Yadav P, Kerkhoff Y, Mittal A, Achazi K, Haag R & Sharma S K, *New J Chem*, 43 (2019) 11984.
29 Mishra B, Barik A, Priyadarshini K N & Mohan H, *J Chem Sci*, 117 (2005) 641.
30 Delley B, *J Chem Phys*, 92 (1990) 508.
31 Delley B, *Phys Review B*, 66 (2002) 155125.
32 Perdew J P, Burke K & Ernzerhof M, *Phys Rev Lett*, 77 (1996) 3865.
33 Weinert M & Davenport J W, *Phys Review B*, 45 (1992) 13709.
34 Andzelm J, King-Smith R D & Fitzgerald G, *Chem Phys Lett*, 335 (2001) 321.
35 Baker J, Kessi A & Delley B, *J Chem Phys*, 105 (1996) 192.
36 Mayer I, *Int J Quant Chem*, 29 (1986) 477.
37 Hirshfeld F L, *Theor Chem Acta*, 44 (1977) 129.
38 Kumar A, Mohan B, Modi K, Din M A & Kumar S, *J Molecular Struct,* 1268 (2022) 133609.
39 Diallo M S, Christie S, Swaminathan P, Johnson J H & Goddard W A, *Environ Sci Technol*, 39 (2005) 1366.
40 Camci-Unal G & Pohl N L B, *Carbohydr Polym*, 81 (2010) 8.
41 Shortreed M, Kopelman R, Kuhn M & Hoyland B, *Anal Chem*, *68* (1996) 1414.
42 Caballero A, Martínez R, Lloveras V, Ratera I, Vidal-Gancedo J, Wurst K, Tárraga A, Molina P & Veciana J, *J Am Chem Soc*, 127 (2005) 15666.
43 Lin W, Yuan L, Long L, Guo C & Feng J, *Adv Funct Mater*, 18 (2008) 2366.
44 Zhou L, Russell D H, Zhao M & Crooks R M, *Macromolecules*, 34 *(*2001) 3567.
45 Knecht M R, Garcia-Martinez J C & Crooks R M, *Chem Mater*, 18 (2006) 5039.
46 Bakshi R, Rossi M, Caruso F & Mathur P, *Inorg Chem Acta*, 376 (2011) 175.
47 Babu M S S, Reddy K H & Krishna P G, *Polyhedron*, 26 (2007) 572.